

Measurement of Speed of Sound Using Transmitter-Receiver Time and a Resonance Tube

Harry Yamada (260921249), Kusha Sareen (260906331), Felix Gottlieb
(260918881), Simon Overgaard (260925648)

McGill University Department of Physics

May 11, 2022

Abstract

The speed of sound is relevant to many technologies, from the design of musical instruments to sonar detection and communication systems. In this paper, two methods for the measurement of the speed of sound are compared. Measuring wave travel time at various distances, the speed $341 \pm 8 \text{ m s}^{-1}$ at $20.8 \pm 0.2 \text{ }^\circ\text{C}$ and 1 atm was determined, consistent with the literature value $344.1 \pm 0.1 \text{ m s}^{-1}$. Using a resonance tube, a speed of $344 \pm 1 \text{ m s}^{-1}$ at $21.8 \pm 0.2 \text{ }^\circ\text{C}$ and 1 atm was determined, in accordance with the accepted value $344.7 \pm 0.1 \text{ m s}^{-1}$. Ultimately, the resonance tube method proved to be more robust, producing a lower error bound.

1 Introduction

Following the discovery of the wave-like nature of sound in the 17th century, physicists began making attempts to measure its speed. The speed of sound remains relevant to many modern-day technologies, from sonar detection and communication to designs of sound systems and wind instruments. Its value, 343 m s^{-1} at $20 \text{ }^\circ\text{C}$, has historically been of interest and many methods have been employed to find it [1]. This experiment utilizes two such approaches. In the first, high precision computer clocks and a microphone are used to measure the time between sound transmission and reception at variable distances. In the second, a tone with ramping frequency is played into a resonance tube to determine the resonance peaks.

2 Transmission-Reception Time

2.1 Background

This part of the experiment will measure the speed of sound from first principles, emitting a tick sound and measuring the amount of time it takes to reach a receiver a given distance away. The dependence of transmission-reception time Δt on distance Δd is expected to be,

$$\Delta t = \frac{\Delta d}{v} + \tau, \quad (1)$$

where v [m/s] is the speed of sound and τ [s] is the onset latency associated with signal processing at the level of the speaker, microphone and audio software. A linear fit of transmission-reception time Δt to distance Δd will yield the speed v by the slope. The magnitude of the onset delay τ is irrelevant to the measurement; however, it is essential to ensure the variance in this quantity is small between trials to minimize the systematic error.

2.2 Materials and Methods

Figure 1 depicts the experimental apparatus. Temperature was measured to be $20.8 \pm 0.2 \text{ }^\circ\text{C}$ using 5 trials with a thermometer. A tape measure precise to 0.1 cm was used to measure straight-line unobstructed microphone-to-speaker distances. Using Audacity, a tick noise

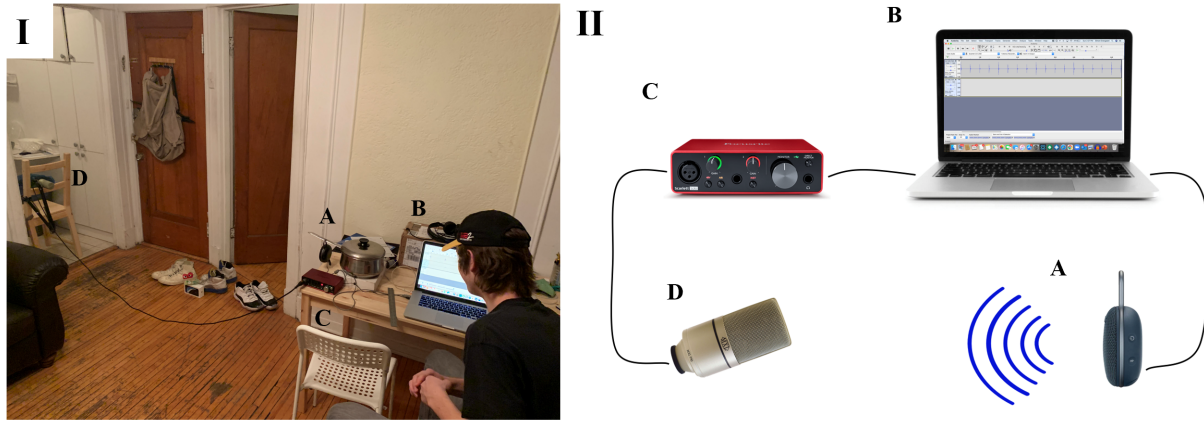


Figure 1: (I) Photo of experimental setup. (II) A clearer schematic of the apparatus. Consists of JBL Clip 3 speaker attached to a saucepan (A), 2015 MacBook Pro running Audacity (B), Focusrite interface (C) connected to MX 990 microphone (D) fixed to a wooden chair, attached to speaker via AUX.

was generated through the speaker and registered by the microphone. A sampling rate of 8000 Hz for the recorder was used to minimize the variance in onset delay τ resulting from computational time. Given Audacity records and plays audio simultaneously, both audio tracks (generating and recording) are synchronized at $t = 0$, and any variation due to the equipment is accounted for by the variance in τ . Gain was adjusted to ensure signal onset was clearly apparent within one sample (see Appendix A). Eleven measurements at each distance were taken at 14 different distances, ranging from 0 to 2.6 metres.

2.3 Results

Figure 2 depicts the distribution of transmission-reception time measurements at 30.48 cm and a linear plot of average time Δt at varying distances. A linear fit was used to determine the velocity $341 \pm 8 \text{ m s}^{-1}$.

The reduced chi-squared value is $\chi_r^2 = 1.15$, falling within two standard deviations given 12 degrees of freedom. Fluctuations alone produce this value or lower 69% of the time, suggesting the data is well represented by the model. Additionally, the lack of structure in the residuals suggests the model is sufficient.

An investigation of the systematic uncertainty reveals that precision due to sample rate is the major contributor to the uncertainty in the measured speed. Variance in the signal

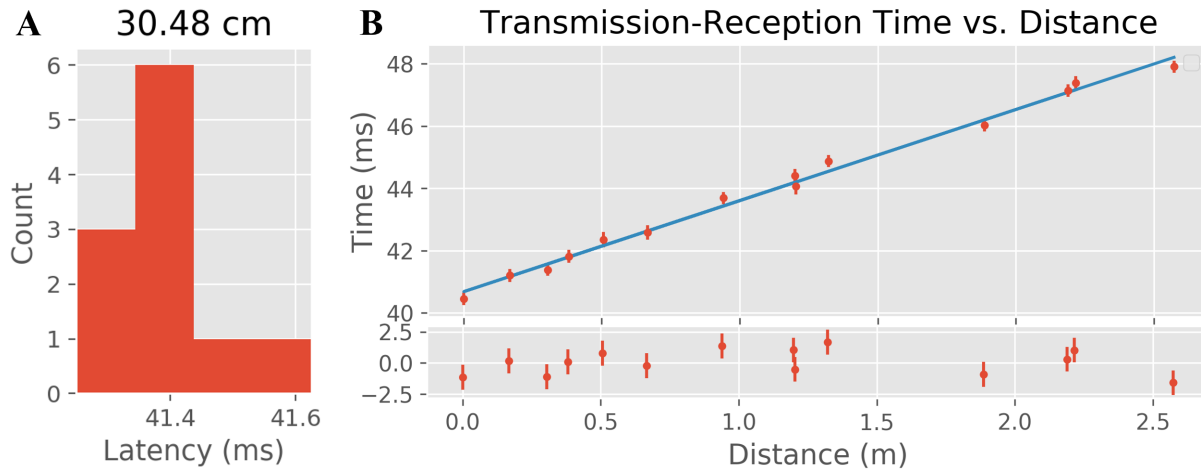


Figure 2: (A) shows a histogram of the transmission-reception time measured at 30.48 cm from the transmitter, (B) shows the average time at each distance fit to a line with Studentized residuals. Fit parameters for Equation 1, the line $\Delta t = \frac{\Delta d}{v} + \tau$, are $\tau = 40.7 \pm 0.1$ s and $v = 341 \pm 8$ m s⁻¹ ($\frac{\chi^2}{dof} = 1.15$).

onset delay τ , although also a factor, has a less significant impact on the measurement.

2.4 Discussion

The accepted value for the speed of sound at 20.8 ± 0.2 °C is 344.1 ± 0.1 m s⁻¹. Thus, our measurement agrees with the accepted value within error bounds.

A key contributor to the measurement error was the variance in the onset delay of the recording system τ . This was minimized by lowering the sampling rate, but a delay of 40.5 ± 0.3 ms was measured regardless. It is expected that sound should take approximately 3 ms to travel about 1 meter so this is a significant contribution. Taking multiple trials results in an improvement and we found a standard error of about 0.08 ms at a given distance. A low sampling rate, however, limits the accuracy to which the onset of the signal can be measured. As shown in Appendix A, the onset of the sound is characterized by a sample with clear deviance from zero and association to a waveform. For instance, at 8000 Hz, there is a 0.13 ms delay between samples. The sampling rate of 8000 Hz was chosen to minimize the total systematic uncertainty introduced by these two effects.

Additionally, uncertainty relating to the audio equipment used, uncertainty in the distance measurement, and the uncertainty in the angles of the microphone and speaker also play a

role. Measures were taken to ensure the best possible straight line measurement was taken. The particulars of the audio equipment are all accounted for in τ . The uncertainty in the tape measure was accounted for by taking multiple measurements, but it was concluded that error of half a tick mark (0.5 mm) could not be improved.

Additional trials were conducted to determine the impact of microphone rotation on the measured sample counts. It was found that at $\Delta d = 30.5$ cm, a 45-degree offset decreased the average transmission-reception time by 0.063 ms (See Appendix E). This gives an upper bound on the error associated with angle, since the angles should vary much less than 45 degrees in the trials, which is accounted for as part of the systematic uncertainty.

Finally, the impact of atmospheric conditions on the speed of sound is another consideration. Air pressure is known not to impact the speed of sound to the first order in an ideal gas [2]. A Taylor expansion at 295.15° Kelvin (22 °C) of the accepted formula for speed of sound as a function of air temperature, shows the speed of sound varies by about 0.6 m/s per degree [3]. Thus, it is important to consider this discrepancy when comparing to literature values obtained in similar, but slightly different atmospheric conditions. This bound is well contained within the error estimate for our measurement.

This method, much like any experiment aiming to measure a large velocity over a short distance, has a greater error bound than literature values. However, we obtain a more precise measurements than some other experiments with the same methodology (see [4]). In future experiments, using a computational interface/microphone with a lower variance in its onset delay at a greater sampling frequency and measuring over a greater distance would improve the measurement.

3 Resonance Tube

3.1 Background

Sound produces transverse waves as it travels, resulting in deviations in air pressure. Playing a sound into a tube at specific frequencies related to its length results in large amplitude standing waves in the tube of that given frequency, a process called resonance. The expression

for air overpressure p_n - pressure greater than atmospheric - for the n^{th} harmonic in a tube of length L with respect to space x and time t is given by the standing wave equation

$$p_n(x, t) = P_n \cos \frac{n\pi x}{L} \cos w_n t, \text{ for } w_n = \frac{n\pi v t}{L}, \quad (2)$$

where P_n [Pa] is the amplitude of the n^{th} harmonic, w_n [Hz] is the resonance angular frequency and v [m/s] is the speed of sound [5].

In a closed-end tube, only odd harmonics are able to exist, since the air pressure at the closed end is necessarily of greatest amplitude and pressure is equal to atmospheric at the open end. As a result, the gap between resonance frequencies Δf is given by [6]

$$\Delta f = \frac{v}{2L}. \quad (3)$$

In a non-ideal tube, however, the standing wave at resonance is not fully contained in the tube. As such, end correction must be performed to the measured tube length L_m according to

$$L = L_m + L_e \text{ for } L_e = 0.6 \times r, \quad (4)$$

where L_e is the corrected end of the tube and r is the tube radius [7].

3.2 Materials and Methods

Figure 3 depicts the experimental apparatus at 21.8 ± 0.2 °C. Frequency of a tone emitted by the Audacity Waveform Generator was linearly increased from 300 Hz to 1200 Hz over a period of 30 seconds in ten trials. A long narrow resonance tube was used to minimize the necessary end correction (Equation 4) and ensure many resonance peaks of measurable amplitude were observed over the playable frequency range. The microphone sampling rate was maintained at 8000 Hz and amplitude of the signal resonating in the tube was recorded. The microphone was placed directly behind the speaker as this location produced the clearest and most discernible resonance peaks. Testing revealed the position of the microphone did not impact the inter-resonance peak interval Δf but did impact the clarity of the resonance

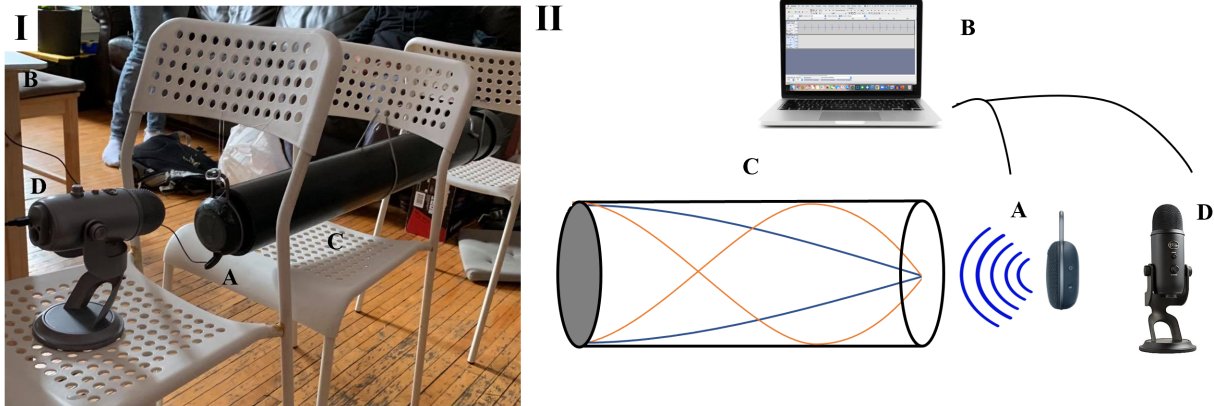


Figure 3: (I) Photo of experimental setup. (II) A clearer schematic of the apparatus. Consists of JBL Clip 3 speaker (A), 2015 MacBook Pro running Audacity (B), a 93.50 ± 0.05 cm long by 10.00 ± 0.05 cm diameter PVC pipe (C), and a Blue Yeti USB microphone (D).

peaks. Peaks were picked by a Python script (see Appendix D) and the inter-resonance peak interval was used to determine the wave speed according to Equation 3.

3.3 Results

For each of ten trials, the intervals between the picked peaks (shown in Figure 4) were averaged. A weighted mean of each trial was taken to produce a final value of $\Delta f = 178.1 \pm 0.7$ Hz. Uncertainty for the length and diameter of the tube were 0.05 cm, half the spacing between ticks on the measuring tape. The temperature was determined over 5 trials. Using Equation 3, the speed of sound was determined to be 344 ± 1 ms^{-1} .

An investigation of the systematic and statistical uncertainties reveals that the variation in the inter-resonance peak intervals is the major contributor to the uncertainty in the measured speed. Uncertainty in the length of the tube, or more precisely the length of the standing pressure wave contained in the tube, is also a contributor but is much less significant.

3.4 Discussion

The accepted value for the speed of sound at 21.8 ± 0.2 °C is 344.7 ± 0.1 ms^{-1} . Our value of 344 ± 1 ms^{-1} is in agreement.

Unlike the first method, uncertainty in measured distances is more directly relevant, as the speed of sound is fairly sensitive to the length of the resonance tube. As for frequency

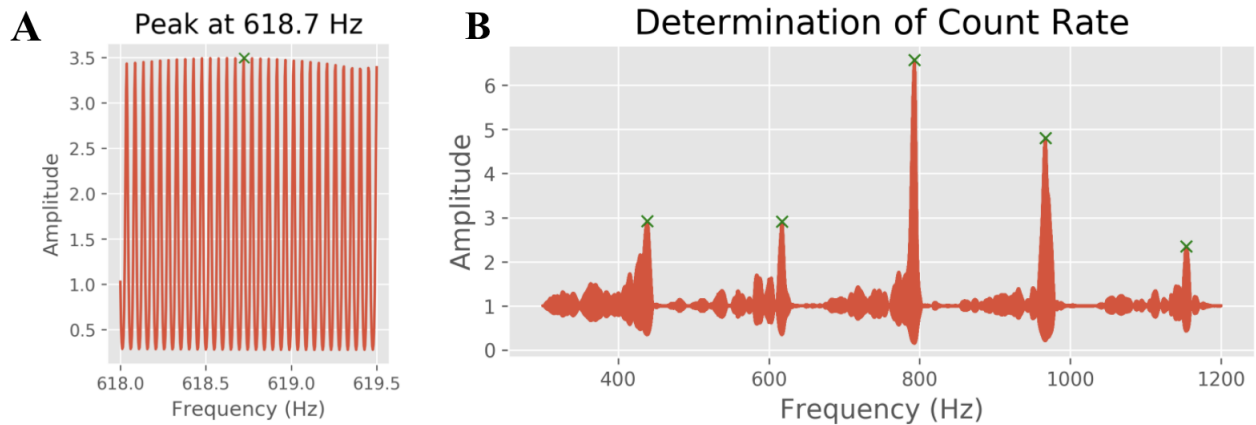


Figure 4: (A) Zoomed into a peak picked at 618.7 Hz, showing the sinusoidal shape of the waveform. (B) Waveform amplitude measured over 30 seconds, ramping the frequency from for a given trial.

measurements, the uncertainty associated with the sample rate, 0.004 Hz, is inconsequential relative to the statistical uncertainty on each trial. The statistical uncertainties were taken to be the standard error in the mean over the four peak-to-peak distances, and generally sat in the range of 2-4 Hz. These two uncertainties were propagated through to the weighted mean of frequency, and eventually the speed of sound, in tandem with the length uncertainty of 0.0522 cm, 0.0022 cm of this coming from end correction.

Choosing a sampling rate of 8000 Hz here is sufficient as it fulfills the Nyquist criterion, no aliasing occurs in the signal, and it minimizes the delay between a frequency being played and the resonance being measured in the microphone [8]. The experiment is designed such that the absolute resonance frequency is not important but the gap between frequencies, Δf , is. As such, the absolute magnitude of this delay isn't important but rather, as with the transmission-reception time method, its variance is. As before, sampling at 8000 Hz minimizes this variance.

We conclude that this method produces a more accurate and precise measurement than the first. Introduction of a resonance tube makes the measurement far more robust. This experiment, like the first, allows us ignore the onset latency introduced by any equipment and, thus, minimize the systematic error significantly. Unlike the first, however, the tube produces resonance peaks that can be measured to a far lower percent error than travel time

of sound.

We favour this method of linearly ramping frequency over a given interval in contrast to changing the effective length of the tube (as seen in [9]) as we minimize the impact of length measurements of the tube - the key contributor to error in most resonance tube experiments - and have an experimental apparatus with very few moving parts. In future experiments, taking more trials to minimize the statistical uncertainty in the inter-resonance peak interval would be expected to improve the measurement. Additionally, sampling over a greater frequency range or using a longer tube, allowing for more resonance peaks in a given frequency range, would further decrease statistical uncertainty.

4 Conclusions

Two methods for the measurement of the speed of sound were compared. Using wave travel time at various distances, the speed $341 \pm 8 \text{ m s}^{-1}$ at $20.8 \pm 0.2 \text{ }^\circ\text{C}$ and 1 atm was measured, consistent with accepted literature value $344.7 \pm 0.1 \text{ m s}^{-1}$. Using a resonance tube, the speed was found to be $344 \pm 1 \text{ m s}^{-1}$ at $20.8 \pm 0.2 \text{ }^\circ\text{C}$ and 1 atm, consistent with the accepted value at this temperature, $344.1 \pm 0.1 \text{ m s}^{-1}$. The resonance tube method produces a measurement more robust to systematic error than the transmission-reception time method. Collecting data at greater distances and utilizing more efficient software could improve the transmission-reception method, while the resonance tube method could be augmented with a longer tube, larger frequency range, or, ultimately, more data.

References

- [1] N. Zizawitz and M. Davids, *Physics: Principles and Problems*. New York: Glencoe, 1995. 1
- [2] R. Nave, “Speed of sound,” August 2000. [Online]. Available: <http://hyperphysics.phy-astr.gsu.edu/hbase/Sound/souspe3.html> 4
- [3] T. Brice and T. Hall, Apr 2020. [Online]. Available: https://www.weather.gov/epz/wxcalc_speedofsound 4
- [4] M. Bin, “Measuring the speed of sound using only a computer,” *The Physics Teacher*, vol. 51, no. 5, pp. 295–297, 2013. 4
- [5] N. Rinaldo, Martin and Woodman, “Standing waves,” 11 2020, online; accessed 2021-04-08. [Online]. Available: <https://phys.libretexts.org/@go/page/19467> 5
- [6] R. Nave, “Air column resonance,” August 2000. [Online]. Available: <http://hyperphysics.phy-astr.gsu.edu/hbase/Waves/opecol.html> 5
- [7] M. J. Ruiz, “Boomwhackers and end-pipe corrections,” *The Physics Teacher*, vol. 52, no. 2, pp. 73–75, 2014. [Online]. Available: <https://doi.org/10.1119/1.4862106> 5
- [8] M. H. Weik, *Nyquist criterion*. Boston, MA: Springer US, 2001, pp. 1127–1127. [Online]. Available: https://doi.org/10.1007/1-4020-0613-6_12649 7
- [9] G. J. Howgate and K. D. Pithia, “Calculation of the velocity of sound using a resonance tube,” *Physics Education*, vol. 53, no. 6, p. 063006, oct 2018. [Online]. Available: <https://doi.org/10.1088/1361-6552/aae26e> 8

5 Author Contribution

Writing and analysis were split evenly between all parties in all sections of the lab.

6 Appendix

A Raw Audacity Waveform

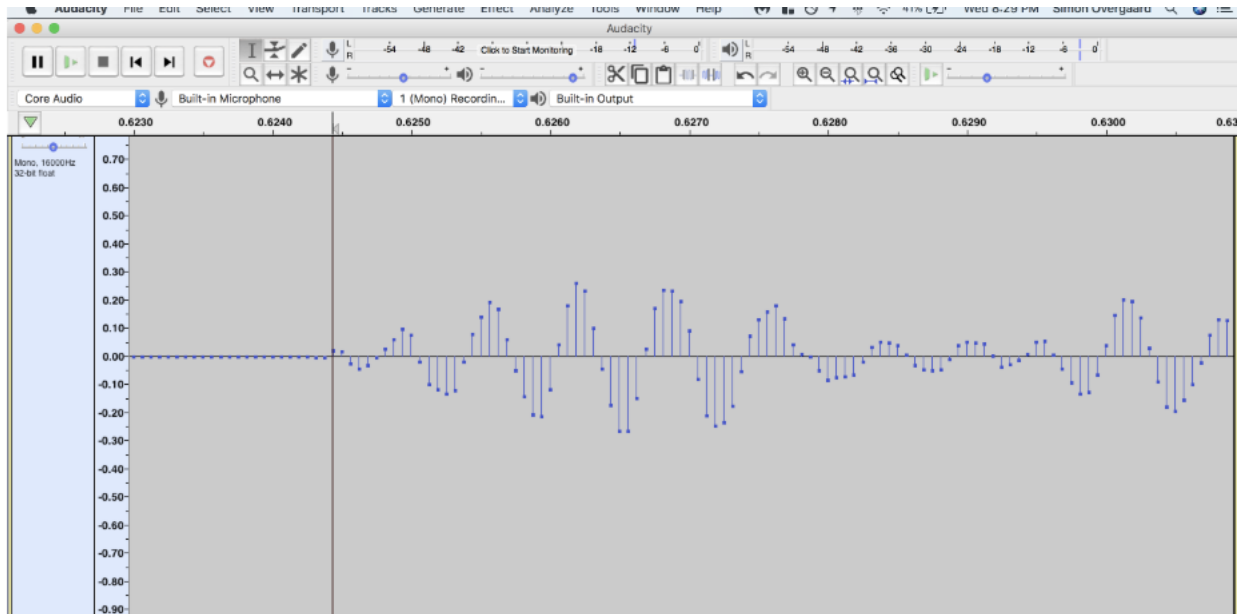


Figure 5: Signal onset in Audacity Environment.

B Sample Data for Transmission-Reception

Trial no.	Counts
1	355 \pm 1
2	351 \pm 1
3	355 \pm 1
4	352 \pm 1
5	351 \pm 1
6	353 \pm 1
7	350 \pm 1
8	352 \pm 1
9	351 \pm 1
10	354 \pm 1
11	354 \pm 1

Table 1: Sample data taken at $\Delta d = 120.33$ cm

C Mean Peak-to-Peak Values

Trial no.	Mean (Hz)	Standard err (Hz)
1	179	3
2	179	2
3	175	1
4	178	2
5	179	3
6	178	2
7	179	3
8	177	2
9	179	3
10	179	3

Table 2: Mean peak-to-peak frequency intervals from method 2, with standard error in mean.

D Pseudocode for Peak-Picking Algorithm

```
highest = 0;
peaks = [];
freqs = [];
//find local maxima above a certain threshold amplitude
for sample in TimeSeries:
    if (sample.ampl > threshold) && (sample.ampl > highest){
        highest = sample.ampl;
        peaks.append(sample.ampl);
        freqs.append(sample.freq);
    }
    if threshold - 0.05 < sample.ampl < threshold + 0.05 {
        highest = 0.05;
    }
i = 0;
// clean up the pool of peaks so that only the highest peaks in each cluster are considered
while i != peaks.length() {
    if peaks[i] < peaks[i+1] && freqs[i+1] - freqs[i] > 100:
        peaks.remove(peaks[i]);
        freqs.remove(freqs[i]);
    }
    else i++;
}
```

Figure 6: Pseudocode for the peak-picking algorithm. The "threshold" value (usually 2.5 or 3) was changed to tailor to each dataset to optimize runtime, as the peak amplitudes varied set-to-set.

E Investigating the Effect of Angle on Latency

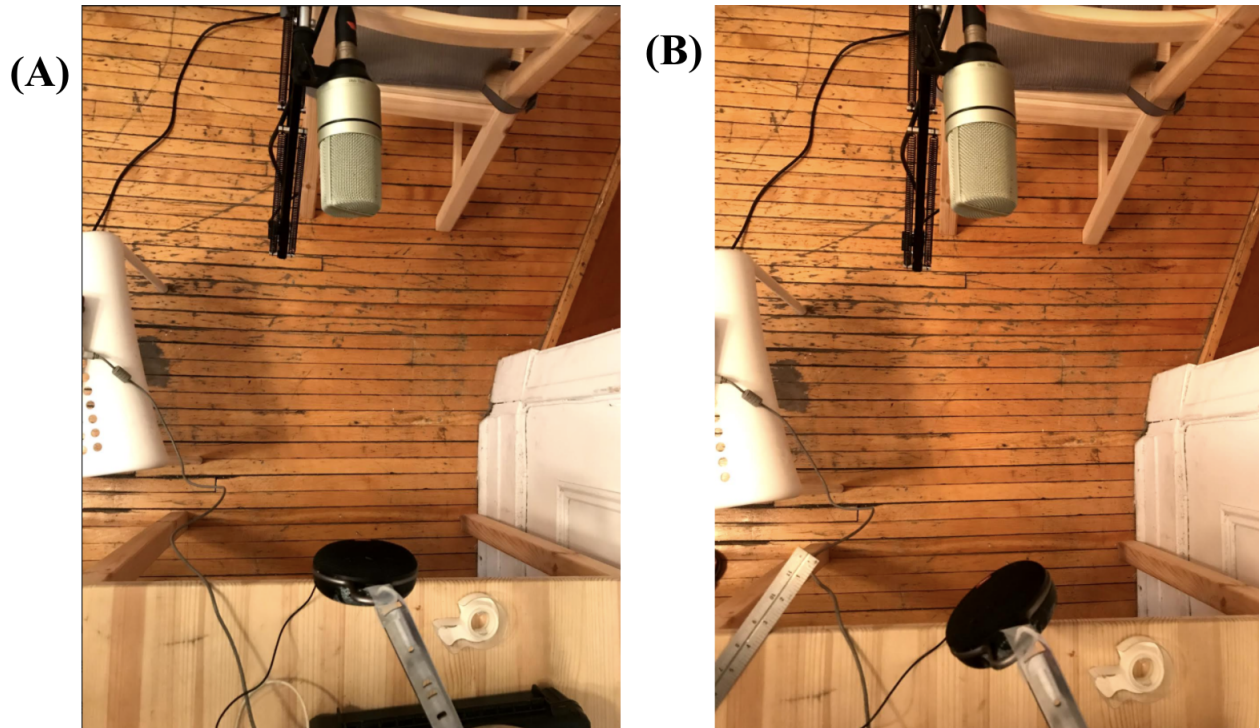


Figure 7: Apparatus of trials taken at a 0-degree shift (A) and 45-degree shift (B).

	Mean Counts	Standard Deviation
0 Degrees	334.0	1.095
45 Degrees	333.5	1.285

Table 3: Data from eleven trials at each angle.